Water Research 132 (2018) 260–269

Contents lists available at ScienceDirect

Water Research

journal homepage: www.elsevier.com/locate/watres

Speciation evolution of zinc and copper during pyrolysis and hydrothermal carbonization treatments of sewage sludges

Rixiang Huang, Bei Zhang, Emily M. Saad, Ellery D. Ingall, Yuanzhi Tang*

School of Earth and Atmospheric Sciences, Georgia Institute of Technology, 311Ferst Dr, Atlanta, GA 30324-0340, USA

ARTICLE INFO

Article history:
Received 17 September 2017
Received in revised form
10 December 2017
Accepted 3 January 2018
Available online 4 January 2018

Keywords:
Sewage sludge
Pyrolysis
Hydrothermal carbonization
Heavy metals
Speciation

ABSTRACT

Thermal and hydrothermal treatments are promising techniques for sewage sludge management that can potentially facilitate safe waste disposal, energy recovery, and nutrient recovery/recycling. Content and speciation of heavy metals in the treatment products affect the potential environmental risks upon sludge disposal and/or application of the treatment products. Therefore, it is important to study the speciation transformation of heavy metals and the effects of treatment conditions. By combining synchrotron X-ray spectroscopy/microscopy analysis and sequential chemical extraction, this study systematically characterized the speciation of Zn and Cu in municipal sewage sludges and their chars derived from pyrolysis (a representative thermal treatment technique) and hydrothermal carbonization (HTC; a representative hydrothermal treatment technique). Spectroscopy analysis revealed enhanced sulfidation of Zn and Cu by anaerobic digestion and HTC treatments, as compared to desulfidation by pyrolysis. Overall, changes in the chemical speciation and matrix properties led to reduced mobility of Zn and Cu in the treatment products. These results provide insights into the reaction mechanisms during pyrolysis and HTC treatments of sludges and can help evaluate the environmental/health risks associated with the metals in the treatment products.

1. Introduction

Management of sewage sludge is a challenging task for the wastewater treatment industry because of the high water content, large volume, and the presence of organic and inorganic contaminants such as heavy metals, pesticides, herbicides, pharmaceuticals and personal care products (PPCPs), and pathogens (Rogers, 1996; Westerhoff et al., 2015). On the other hand, sludges also contain large amounts of energy (i.e., carbon, C) and nutrients (i.e., nitrogen, N, and phosphorus, P) and have great potential for resource recovery (Koppelaar and Weikard, 2013; Withers et al., 2015). However, current waste management strategies have intrinsic problems that result in limited resource utilization of sludges. In the United States, ~35% of the sewage sludges are recycled in agriculture, ~30% are disposed in landfill, ~15% are thermally disposed, and the rest are disposed by other means (Christodoulou and Stamatelatou, 2016). High landfill disposal costs associated with transport and land availability make this option less favorable. Strict regulations inhibit direct land application of sludges due to concerns with soil contamination and related environmental and human health risks (Christodoulou and Stamatelatou, 2016). With the global interests in societal and environmental sustainability, there are urgent needs for the integration of new technologies and strategies into current sludge management systems (Spinosa, 2004; Wang et al., 2015).

In recent years, thermal and hydrothermal treatments of sewage sludges have emerged as sustainable treatment techniques, because they have the potential to simultaneously target environmental protection, energy recovery, and nutrient recovery/recycling (Barber, 2016; Wang and Li, 2015). These treatments can degrade pathogens, decompose organic contaminants, and reduce waste volume, thus serving as excellent sanitation and waste management options (Escala et al., 2012; vom Eyser et al., 2015a; vom Eyser et al., 2015b). Two representative thermal and hydrothermal treatment techniques are pyrolysis and hydrothermal carbonization (HTC), respectively. The treatment products (chars, including pyrochar from pyrolysis and hydrochar from hydrothermal treatments) are potential stand-alone fuel sources (Bridle and Pritchard, 2004; Kim et al., 2014b; Zhao et al., 2014). Chars can also be applied as soil amendments for contaminant remediation, for improving soil quality, or as fertilizers (Atkinson et al., 2010;

* Corresponding author.
E-mail address: yuanzhi.tang@eas.gatech.edu (Y. Tang).

https://doi.org/10.1016/j.watres.2018.01.009
0043-1354/

Hossain et al., 2010; Malghani et al., 2013). Overall, applications of thermal and hydrothermal techniques have strong potential in mitigating the environmental burdens of sludge management and enhancing societal sustainability.

Properties and functionality of the treatment products are largely governed by the composition and speciation of elements embedded. The concentration and speciation of heavy metals are relevant to environmental risks associated with the disposal and applications of sludge-derived products, since heavy metal speciation largely determines their mobility and availability (Lake et al., 1984; Reeder et al., 2006). Many previous studies have examined the behavior of heavy metals during thermal and hydrothermal treatments of sludges, primarily focusing on heavy metal phase distribution (in solid, liquid, and gas phases), or mobility/transformation using empirically defined sequential chemical extraction methods (Huang & Yuan, 2016; Jin et al., 2016; Leng et al., 2014; Li et al., 2012; Shao et al., 2015; Shi et al., 2013; Wu et al., 2016; Yuan et al., 2011, 2015; Zhang et al., 2016). However, chemical extraction is an indirect method and the obtained fractions do not necessarily correlate with the chemical species targeted by a specific extraction step. Metal reaction with the extracting solutions can also potentially cause alterations or transformations of metal speciation.

Much still remains unknown on the detailed speciation of heavy metals and the effects of treatment conditions during thermal and hydrothermal treatments of sludges. Heavy metals in sludges can exist in diverse physical and chemical forms. For example, Cu and Zn were found to exist as sulfides, phosphates, organic-complexes, and iron mineral associated species with sizes ranging from nano- to micrometers (Donner et al., 2011, 2012; Kim et al., 2014a; Lombi et al., 2012; Ma et al., 2014a). Synchrotron based X-ray absorption spectroscopy (XAS) is a non-destructive technique that can provide detailed metal speciation information in complex heterogeneous environmental samples. By combining XAS and sequential extraction, one can potentially obtain in-depth information on metal speciation and mobility that cannot be achieved by sequential chemical extraction alone. Although recent studies have characterized Cu and Zn speciation transformation during traditional treatments (such as aging, chemical amendments, and anaerobic digestions) using these techniques (Donner et al., 2011, 2012; Legros et al., 2017), little is known about the transformation of these species during thermal and hydrothermal treatments.

In this study, activated and anaerobically digested sewage sludges from a municipal wastewater treatment plant were treated with pyrolysis and HTC at different temperatures. As previously discussed, pyrolysis and HTC are representative thermal and hydrothermal techniques, respectively, and their applications to sludge treatment have been extensively studied (Escala et al., 2013; Manara and Zabaniotou, 2012; Wang et al., 2014). The speciation and mobility of Cu and Zn, two abundant heavy metals in sewage sludges, were characterized using sequential extraction, bulk X-ray absorption spectroscopy (XAS), and coupled micro-X-ray fluorescence (μ-XRF) imaging and absorption spectroscopy (μ-XAS). Particularly, the use of microanalysis enabled the characterization of particulate forms of these metals and cross-validation of bulk analysis. Results from this work can improve our understanding of the thermochemical behaviors of these elements in sludges, and also provide fundamental information for evaluating heavy metal mobility and environmental risks when the treatment products are applied.

2. Experimental approaches

2.1. Sample collection

Sewage sludges were collected from F. Wayne Hill Water Resources Center (Gwinnett County, Atlanta, GA, USA), which collects and treats municipal sewage from the County. This treatment plant has primary (physical), secondary (activated sludge), and tertiary (membrane filtration and ozonation) treatment units. 10 ppm of Al is added to the clarifiers to facilitate sludge aggregation and settling, and 25 ppm of $FeCl_3$ is added in the tertiary process for phosphate removal. Excess activated sludge and sludge from primary treatment unit are combined into anaerobic digester for biogas production, and most of the biosolids are disposed in landfill. Activated sludge is the excess sludge from the secondary clarifier, and anaerobically digested sludge (hereafter referred to as anaerobic sludge) was collected from the outlet of anaerobic digester. The activated sludge was further enriched by centrifugation and stored at −20 °C, while the anaerobically digested sludge was stored at −20 °C without pretreatments. For pyrolysis, a portion of the samples was freeze dried before treatments. For HTC, frozen samples were thawed at room temperature prior to treatments.

2.2. Pyrolysis and HTC treatment of sludges

Pyrolysis of the sewage sludges was performed in a quartz tube furnace (Thermo Scientific, MA, USA) under N_2 flow (~1 mL/s) at 250 and 450 °C, with a heating and cooling rate of 200 °C/h and a duration at the target temperature of 4 h. These two temperatures represent the low and middle temperature range of thermal treatments, at which mass remains mostly in solid phase (Table 1). Although low temperature pyrolysis treatment is also known as torrefaction, for simplicity, treatments at both temperatures are hereafter referred to as pyrolysis. For each treatment condition, freeze-dried sludges (1.0 g) was added to a crucible and inserted into the glass tube. The products are referred to as pyrochars. HTC treatments of both sludges were performed in the presence of deionized water (DI) with a solid:liquid ratio of 1:9 (w/w) and pH around 6.6. To achieve this, 4 g of the sludges (equivalent to ~1 g dried mass) and 6 g DI water were mixed in a 20 mL Teflon lined stainless steel hydrothermal reactor (Parr instrument, IL, USA). The reactor was sealed and heated in an oven at 175 or 225 °C for 16 h, then allowed to cool down to 50 °C overnight in an oven. Solid hydrochars produced from HTC were collected by centrifugation and dried at 50 °C for at least 24 h until no further weight loss. All treatments were processed in duplicate.

2.3. Bulk X-ray absorption spectroscopy (XAS)

Cu and Zn K-edge XAS analysis of raw and treated sludge samples and reference compounds were collected at Beamlines 5-BM-D and 12-BM-B at Advanced Photon Source (APS; Argonne National Laboratory, Lemont, IL), and Beamline 4-1 at the Stanford Synchrotron Radiation Lightsource (SSRL; Menlo Park, CA). Energy calibration used the corresponding metal foils (Cu at 8978.9 eV and Zn at 9658.9 eV). Spectra of reference foils were collected simultaneously with sample scans. Freeze-dried raw sludges, pyrochars, or oven dried hydrochars were ground into fine powders and packed into Teflon sample holders covered with Kapton tape. XAS data for these samples were collected in fluorescence mode at room temperature using a Vortex detector (APS 5-BM-D) or a 13 element Ge solid-state detector (APS 12-BM-B and SSRL 4-1).

A large library of reference compounds were prepared and analyzed in transmission mode (for concentrated samples, which were diluted by mixing with boron nitride) or fluorescence mode (for diluted samples). Cu reference compounds include different Cu(I)/(II) sulfide minerals/complexes (i.e., Cu(I)-cysteine complex, Cu_2S, CuS, cubanite, chalcopyrite), Cu phosphate, Cu(II) hydroxide ($Cu(OH)_2$), Cu(II) adsorbed on ferrihydrite, and Cu(II)-humic

Table 1
Pyrolysis and HTC treatment conditions, sample labels, and concentrations of major elements of raw and treated sludges. Solid recovery and solid P content data for pyrolysis treatments were from our previous work (Huang & Tang, 2015, 2016).

Sludge type	Treatment	Condition	Sample label	Solid recovery (%)	C (%)	P (%)	Cu (mg/kg)	Zn (mg/kg)
Activated sludge	Raw	Freeze dried	Sludge	–	35.3 ± 0.4	4.1 ± 0.1	160 ± 9	340 ± 20
	Pyrolysis	250 °C, 4 h	S250	69 ± 6	39.5 ± 0.2	5.7 ± 0.1	230 ± 8	440 ± 60
		450 °C, 4 h	S450	46 ± 1	34.0 ± 0.7	8.9 ± 0.1	320 ± 11	670 ± 9
	HTC	175 °C, 16 h	SHTC175	55 ± 4	37.6 ± 0.4	7.6 ± 0.1	310 ± 23	580 ± 33
		225 °C, 16 h	SHTC225	49 ± 1	37.9 ± 0.8	8.1 ± 0.1	330 ± 5	600 ± 12
Anaerobically digested sludge	Raw	Freeze dried	Ana	–	36.1 ± 1.0	3.3 ± 0.1	240 ± 49	510 ± 25
	Pyrolysis	250 °C, 4 h	A250	69 ± 5	36.5 ± 1.1	4.7 ± 0.1	230 ± 13	620 ± 3
		450 °C, 4 h	A450	47 ± 6	29.8 ± 1.2	7.2 ± 0.2	430 ± 56	960 ± 14
	HTC	175 °C, 16 h	AHTC175	65 ± 4	36.0 ± 1.2	3.7 ± 0.4	200 ± 46	450 ± 13
		225 °C, 16 h	AHTC225	50 ± 5	38.3 ± 0.1	6.1 ± 0.1	330 ± 20	720 ± 52

complex. Zn reference compounds include different Zn sulfide minerals/complexes (i.e., Zn-cysteine complex, ZnS, sphalerite, wurzite), Zn phosphate (hopeite $Zn_3(PO_4)_2 \cdot 4H_2O$), Zn(II) associated with Fe oxides (i.e., Zn(II)-sorbed and Zn(II)-doped ferrihydrite), and Zn(II)-humic complex. Details on the reference compounds are provided in Supporting Information (SI) Table S1.

2.4. Micro X-ray fluorescence (μ-XRF) imaging and μ-XAS analysis

Synchrotron μ-XRF imaging and μ-XAS analysis were conducted on raw and treated samples at SSRL Beamline 2–3. Dried samples were gently disaggregated and spread on Kapton tapes. Excess powders were gently blown off. Sample-loaded tapes were mounted on a sample stage and raster-scanned under the beam at an energy of 12 KeV and beam size of 5 μm by 5 μm. At selected hot spots (i.e., locations with high signals of element of interest), Cu and Zn K-edge μ-XANES spectra were collected to reveal the structural information. Processing of image data used the software SMAK developed by Dr. Sam Webb at SSRL.

2.5. XAS data analysis

XAS data processing and analysis used the softwares SIXpack and Ifeffit (Ravel and Newville, 2005; Webb, 2005). Multiple scans (2–6) were energy calibrated and averaged for further analysis. Principal component analysis (PCA) was conducted on the normalized sample spectra to determine the number of components needed for obtaining reasonable fits. Using the corresponding reference compound spectra library, target transformation (TT) was conducted to determine appropriate candidate compounds. Linear combination fitting (LCF) was conducted on both XANES (−20 to +100 eV) and EXAFS (2.5–11.5 $Å^{-1}$) regions. Combinations of TT-determined candidate compounds were used, and the goodness of fit was determined by R-factor. Fits with smallest R-factors were used.

2.6. Sequential extraction

Both raw sludges and their chars were subjected to sequential extraction using the three-step Community Bureau of Reference (BCR) procedure (Mossop and Davidson, 2003). Briefly, 250 mg of dried solids were added to 50 mL polypropylene centrifuge tubes, and sequentially extracted with the following steps: (1) soluble/exchangeable fraction: 20 mL acetic acid (0.11 M) for 16 h, (2) reducible fraction: 20 mL hydroxylamine hydrochloride (0.1 M, pH 2.0) for 16 h, and (3) oxidizable fraction: 4 mL H_2O_2 (30%), air dried, then 20 mL ammonium acetate (1 M, pH 2.0). A portion of the extracted liquids were mixed with certain amount of scandium solution (equivalent to 50 ppb in the final dilution, served as internal standard) and digested by a mixture of concentrated H_2O_2 and HNO_3 (v/v = 1:1) on a hot plate at 100 °C, then diluted for final analysis by inductively coupled plasma–mass spectrometry (ICP-MS). The untreated solids and extracted solid residues were ashed in an oven at 550 °C, followed by digestion with aqua regia. A portion of the digested solution was mixed with Sc standard solution and further diluted for concentration analysis. Metal contents in the untreated solids, extracted liquids, and solid residues were determined by ICP-MS on an Agilent 7500a instrument. All extractions were conducted in triplicates.

3. Results and discussions

3.1. Chemical characteristics of the sludges and derived chars

Sludge type, treatment conditions, sample labels, and elemental concentrations are presented in Table 1. Total sulfur content and recovery in the solid phases are presented in Fig. 1. Other compositional information can be found in our previous studies (Huang & Tang, 2015, 2016). In general, anaerobic sludge has higher Cu and Zn concentrations due to the mixing of activated sludge with primary sludge and the volatilization of organic matters during biogas production. Since heavy metals mostly remained in the solid phase after pyrolysis and HTC treatments, their concentrations in the solids have correspondingly increased. Similar trends were also previously observed for P (Huang and Tang, 2015). In general, products from higher treatment temperatures have higher metal

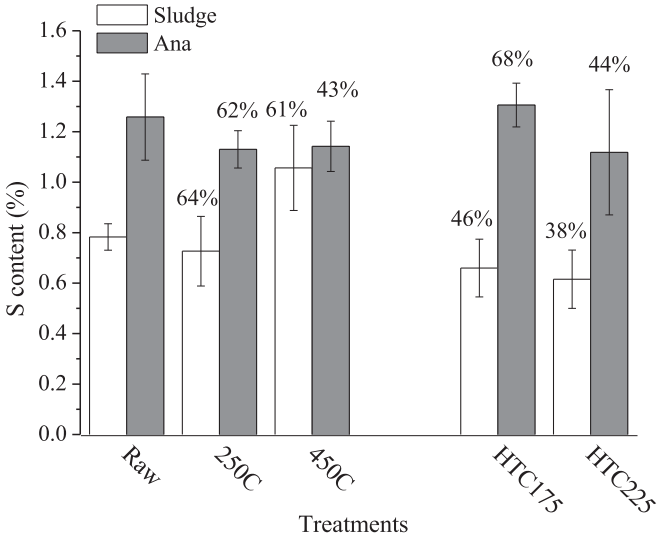

Fig. 1. Changes in the total S content in solid samples and S recovery following pyrolysis and HTC treatments. Numbers are S recovery in the solid phase. Error bars of S content represent standard deviation of measurements (n = 3).

concentrations, as a result of increasing volatilization of organic matter.

3.2. Cu and Zn speciation in raw sludges

Cu and Zn K-edge XANES and EXAFS spectra for the raw sludges and their chars are presented in Fig. 2. LCF was conducted on both XANES and EXAFS data of each sample, and the main difference between these samples is the relative abundance of different sulfide species, which is likely caused by spectral similarities between these species (Tables 2 and SI Table S2). For Cu, the main difference is in the relative abundance of different pure Cu sulfides (cysteine complex, Cu_2S, and CuS) and Cu-Fe sulfides (cubanite and chalcopyrite). For Zn, the main difference is between wurtzite and sphalerite, with LCF of XANES determines more sphalerite, and LCF of EXAFS determines more wurtzite. Wurtzite and sphalerite are two polymorphs of ZnS. Their XANES spectra differ in the white line intensity and post-edge features, with sphalerite having higher white line intensity and sharper post-edge features than those of wurtzite. Regardless of these differences, the trends caused by different treatment techniques and conditions are consistent for both XANES and EXAFS results, therefore discussions in the main text were based on the EXAFS data to avoid redundancy.

Cu exists predominantly as sulfide phases in both sludges, with a small amount as organic complex(es) (fitted as Cu-humic complex) (Fig. 2A and B, Table 2). The sulfide phases identified include organic sulfides (fitted as Cu(I)-cysteine complex), inorganic Cu_2S, and Cu-Fe-sulfide (fitted as cubanite), with pure sulfides constituting 50–60% and cubanite ~ 30% in both sludges. The abundance of Cu(II)-organic complex (fitted as Cu(II)-humic complex) in both samples was similarly low (<15%). Because of the spectra similarity of different Cu-sulfides (e.g., Cu(I)-cysteine complex, Cu_2S, CuS, and cubanite) (Fig. S1), possible overlap between them could occur in LCF, thus they were grouped into sulfide species and their relative abundances were not further interpreted.

For Zn speciation, distinct characteristics were observed comparing the two raw sludges. Spectrum of activated sludge showed higher edge absorption (extended until 9688 eV) and less post-edge features than those of anaerobic sludge (Fig. 2C). The post-edge features (~9679 and 9692 eV) resembled those of Zn

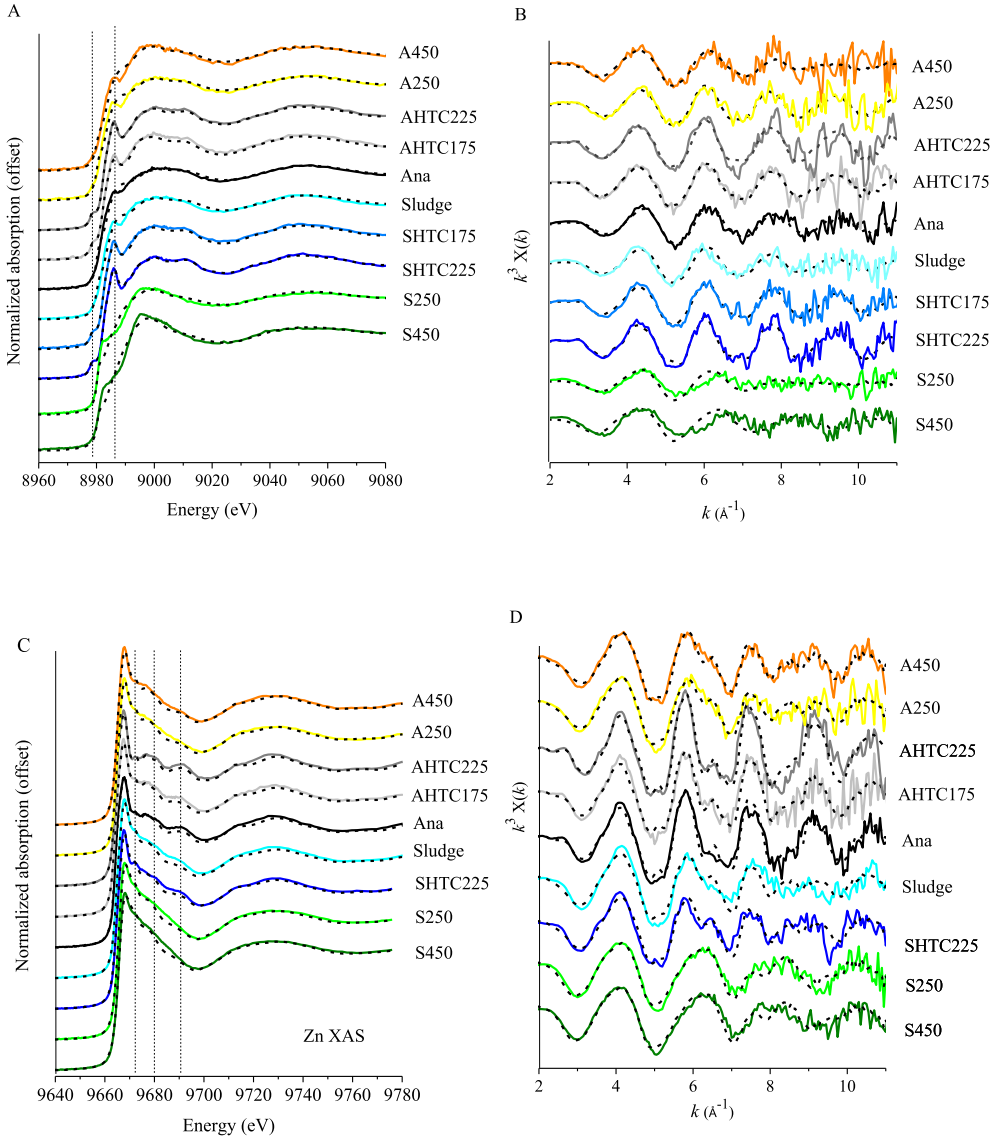

Fig. 2. Cu K-edge XANES (A) and k^3-weighted EXAFS spectra (B), as well as Zn K-edge XANES (C) and k^3-weighted EXAFS spectra (D) of activated sludge, anaerobically digested sludge, and their chars. Raw and LCF fitted data are shown in solid and dashed lines, respectively.

Table 2
Zn and Cu speciation in sludges and their derived chars, determined by linear combination fitting (LCF) of Cu and Zn EXAFS data. Data in the parenthesis are the percentage variation of the fit.

Sample	Cu speciation (%)						Zn speciation (%)			
	Cu_Cys	Cu_2S	Cubanite ($CuFe_2S_3$)	Chalcopyrite ($CuFeS_2$)	Cu_Humic	*R*-factor	ZnS (Wurtzite)	Zn-doped ferrihydrite	Hopeite [$Zn_3(PO_4)_2{\cdot}4H_2O$]	*R*-factor
Sludge	–	50 (19)	35 (11)	–	15 (5.2)	0.45	42 (12)	30 (7.7)	29 (8.6)	0.24
S250	–	63 (9.2)	–	–	37 (19)	0.72	10 (2.3)	56 (7.0)	34 (11)	0.20
S450	–	35 (14)	–	–	65 (22)	0.70	11 (2.2)	43 (6.6)	46 (11)	0.21
SHTC175	–	–	60 (12)	29 (22)	12 (2.9)	0.26	Not measured			
SHTC225	–	–	42 (12)	58 (21)	–	0.18	45 (2.3)	34 (7.0)	22 (7.8)	0.21
Ana	20 (15)	41 (11)	27 (8.8)	–	12 (4.4)	0.31	77 (2.2)	8.3 (3.0)	15 (5.4)	0.12
A250	–	45 (9.1)	55 (14)	–	–	0.34	42 (11)	46 (7.6)	12 (8.6)	0.22
A450	–	24 (17)	37 (13)	–	39 (23)	0.54	51 (0.0)	49 (0.0)	–	0.16
AHTC175	–	–	83 (4.4)	–	17 (4.4)	0.36	71 (3.4)	6.8 (4.6)	23 (6.8)	0.24
AHTC225	–	–	34 (19)	66 (19)	–	0.34	94 (3.0)	–	6.0 (5.8)	0.19

sulfides (Fig. S2). Similar to Cu, a significant fraction of Zn was present as sulfide phases (42% in activated sludge and 77% in anaerobic sludge, Table 2). In addition to sulfides, Zn-phosphate phases (fitted as hopeite) and Zn-associated with Fe oxides (fitted as Zn-doped ferrihydrite) were also present in the raw sludges. Both species accounted for ~30% in activated sludge and <15% in anaerobic sludge.

Elemental composition and speciation in sewage sludges are controlled by a number of factors, such as sewage source, wastewater treatment technology, and sludge processing stage (Donner et al., 2013, 2011, 2012; García-Delgado et al., 2007). Metals in municipal sewage can originate from diverse sources and enter into wastewater treatment plants (WWTPs) in diverse forms (different chemical species in dissolved or particulate states) (García-Delgado et al., 2007; Mitrano et al., 2014; Sterritt and Lester, 1984). During wastewater treatment and sludge production processes, metals can experience extensive transformations, including microbial uptake and utilization, complexation by extracellular substances or minerals, dissolution, and/or precipitation (Brown and Lester, 1982; Chipasa, 2003; Stasinakis et al., 2003; Stephenson and Lester, 1987; Sterritt and Lester, 1984). Since both Cu and Zn are chalcophile elements (i.e., elements with high tendency to combine with sulfur other than oxygen) (Goldschmidt, 1937), it is not surprising to find their dominant association with S, possibly complexed intra- or extracellularly by organic sulfides or precipitated as inorganic sulfides. The relative abundance of different Cu/Zn sulfide phases can be affected by other competing reactions, such as precipitation with phosphate that is found in high concentration in sludges. As shown in a previous study, ZnO nanoparticles (NPs) can be readily transformed into different Zn phosphate solid phases, with the relative abundance of different phases dependent on phosphate concentration and pH (Rathnayake et al., 2014).

Comparison between activated sludge and anaerobic sludge revealed the effects of anaerobic digestion. Higher abundance of metal sulfide species in anaerobic sludge than activated sludge is consistent with the overall higher total S content in anaerobic sludge (Fig. 1). Sulfidation of chalcophile metals during anaerobic digestion of sewage sludges has been previously reported for Ag, ZnO, and CuO NPs (Kim et al., 2015; Lombi et al., 2012, 2013; Ma et al., 2014b). Since most of the Cu already existed as sulfide phases in activated sludge, little alteration occurred for Cu after anaerobic digestion. For Zn, more than half of it was in phosphate phases or associated with Fe, which can be released (via reductive dissolution of Fe phases and dissolution of Zn-phosphates) and precipitate with sulfide species (released from hydrolysis of organic sulfides or from sulfate reduction) (Dunnette et al., 1985; Isa et al., 1986; Lawrence and McCarty, 1965; Legros et al., 2017). Enhanced sulfidation of Cu and Zn was also found in a recent study on anaerobic digestion of different biowastes (Legros et al., 2017).

In addition to bulk XAS analysis, μ-XRF imaging was conducted to reveal elemental distribution and correlations. μ-XANES spectra were collected at Cu and Zn hot spots in the XRF images to identify their speciation within discrete particles (Fig. 3 and Fig. S4). The metals were distributed throughout both activated sludge (Fig. 3 panel A1) and anaerobic sludge (Fig. S4 panel A1), with many scattered particles in micrometer size range and with more Fe-containing particles than Cu- and Zn-containing particles. LCF analyses of Cu and Zn μ-XANES spectra suggests that these particulates are heterogeneous and contain different Cu/Zn species that are consistent with bulk XAS LCF components, consistent with the heterogeneous nature of these samples (data for activated sludge in Table S3 and anaerobic sludge in Table S4).

Sequential extraction results showed that in both activated and anaerobic sludges, Cu existed mostly in the oxidizable fraction (~50%), followed by the residual fraction (20–30%) and reducible fraction (~15%) (Fig. 4). This is consistent with XAS LCF results showing that Cu-sulfides and Cu-humic complexes are the main Cu species. Inorganic Cu sulfides are insoluble in water and weak acid, while their oxidation will result in the dissolution of Cu. Compared to Cu, Zn partitioned mostly in the soluble/exchangeable and reducible fractions (~35% each), less in the oxidizable fraction, and the residual fraction was negligible. A previous study also showed a large fraction of Zn in the soluble/exchangeable fraction (~20–50%) and reducible fraction (30–50%) in a range of sewage sludges (Donner et al., 2011). LCF analyses of XAS data showed that Zn was present mainly as Zn sulfides, Zn-doped ferrihydrite, and Zn-phosphate (as hopeite). Using the geochemical modeling software Phreeqc (Parkhurst and Appelo, 1999), Zn phosphate was calculated to be soluble in the acetic extraction solution, while wurtzite was barely soluble under the same condition. Therefore, Zn in the soluble/exchangeable fraction is likely associated with Zn-phosphate mineral. Zn in the reducible fraction is mostly likely contributed by Zn-doped ferrihydrite, because Zn can be released following the reductive dissolution of Fe(III)-containing minerals. The oxidizable fraction is possibly contributed by Zn-sulfides.

It is worth noting that sequential extraction fractions do not necessarily correlate quantitatively to the relative abundance estimated by XAS fitting. For example, Zn-sulfides are abundant (~40%) based on LCF analyses of EXAFS spectra, while the oxidizable fraction determined by sequential extraction is only ~10%. This could be caused by: 1) potential presence of reference compounds with overlapping spectra features as those used in the LCF of EXAFS data, 2) challenges in including all possible species in the LCF reference library, particularly for highly complex and heterogeneous samples such as sewage sludge, 3) matrix effects that affect the extraction solution chemistry and dissolution kinetics, and 4) speciation alteration during extraction.

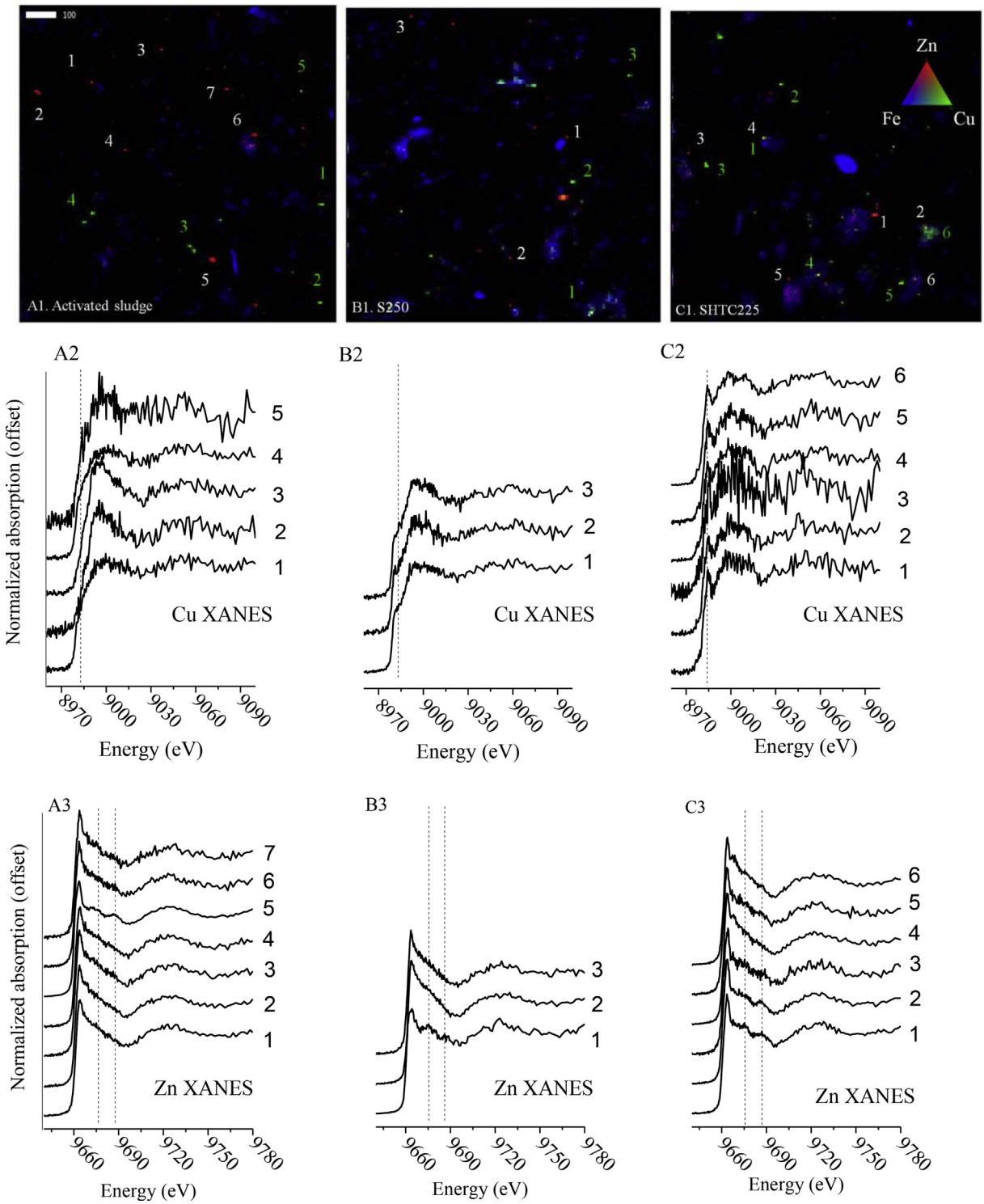

Fig. 3. Tricolor μ-XRF images of Zn, Cu, and Fe distribution in activated sludge (A1), S250 (B1), and SHTC225 (C1). The areas shown are $1 \times 1\ mm^2$ and the scale bar represents 100 μm, with the threshold values set at 50 (Cu), 100 (Zn), and 1000 (Fe). Also shown are the corresponding μ-XANES spectra of Cu (A2, B2, and C2) and Zn (A3, B3, and C3) at different hot spots in the corresponding XRF images. LCF fitting results for these spectra can be found in Tables S3 and S4.

3.3. Effects of pyrolysis on Cu and Zn speciation

Pyrolysis treatment significantly modified Cu and Zn speciation, as shown in the Cu and Zn XANES and EXAFS analyses (Fig. 2, with LCF results in Table 2).

Two main features in the Cu XANES spectra distinguish the raw activated sludge and its pyrochars: decrease of the peak intensity at ~8986 eV and increase of the peak intensity at 8998 eV after pyrolysis. The magnitude of changes also increased with increasing temperature (Fig. 2A). LCF fittings of the pyrochars of activated sludge were less satisfactory (as can be seen and also evidenced by the large R factors), possibly due to the missing of components with

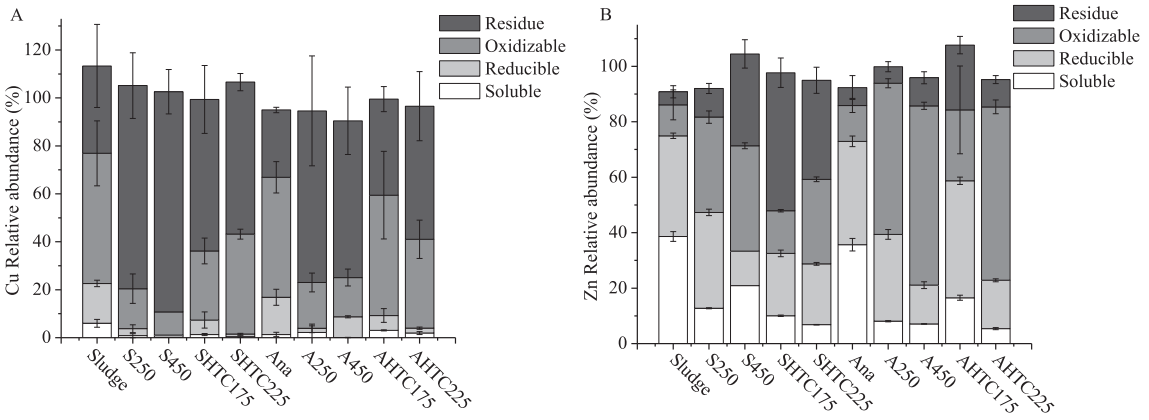

Fig. 4. Distribution of Cu (A) and Zn (B) in the aqueous extracts and solid residue from sequential extraction of the raw sludges and their pyrochars and hyrochars. The relative abundance of Cu/Zn in aqueous extract and the solid residue was calculated by Cu/Zn content in the extract/residue divided by total Cu/Zn content in the solid before chemical extraction (determined by ashing and ICP-MS, the raw data were present in Table S3), error bar represents standard deviation of measurements ($n = 3$).

distorted structures (as shown in the relatively weak oscillations in k space in Fig. 2), or the physical association of Cu phases with the pyrochars (adsorbed species). Nonetheless, LCF fitting of the pyrochars (particularly at 450 °C) suggested a decrease of Cu-sulfide species and an increase of Cu-organic complexes (fitted as Cu-humic complex) (Table 2).

Consistent changes in the Zn XANES spectra features were observed after pyrolysis of both sludges: the post-edge shoulder at ~9672 eV increased while the peak intensity at ~9679 and 9692 eV decreased after treatment (Fig. 2C). Regarding Zn speciation, the primary change is the decrease of Zn-sulfide and the increase of Zn-doped ferrihydrite after pyrolysis (Table 2). After pyrolysis, the abundance of Zn-sulfide in both sludges significantly decreased (from 42 to ~10% and 77 to ~40%, for pyrochars of activated and anaerobically digested sludges, respectively). Zn-doped ferrihydrite increased to 56% (S250) and 43% (S450), compared to 30% in the raw activated sludge. Spectromicroscopy analysis of S250 biochar showed no dramatic changes in the particle morphology and distribution after pyrolysis (Fig. 3 Panels B1-B3), while the speciation of Zn and Cu in corresponding hot spots was transformed and consistent with the bulk speciation evolution (Table S3). Over the tested temperature range (250–450 °C), no effects between these two temperatures were observed for the bulk Zn speciation (Table 2).

The decrease of Cu and Zn sulfides is generally consistent with the volatilization of S during pyrolysis (Fig. 1). As shown in a recent study, 20–60% of the total S was volatized into gas and tar during the pyrolysis of sewage sludge at 100–900 °C, during which H_2S was formed from methanethiol, aliphatic-S, aromatic-S, and thiophene (Zhang et al., 2017). The thermal stability of sulfides is likely phase-dependent and affected by the matrix properties and treatment conditions. Further research is needed to evaluate the thermochemical behaviors of different sulfide species under thermal treatment conditions.

Pyrolysis treatment also significantly altered the mobility of Cu and Zn, in terms of their partitioning in sequential extracts (Fig. 4). After pyrolysis, Cu in all three extractable fractions significantly decreased and migrated into the residual fraction (~80%), and the change was more significant at higher temperature (Fig. 4A). Similar to Cu, the partition of Zn in the soluble/exchangeable fraction was also reduced (from ~35% to ~10%) and the residual fraction slightly increased. The oxidizable fraction increased significantly, from ~10% in raw sludges to ~35%–60% in the pyrochars (as compared to the decrease of this fraction for Cu). The immobilization of Cu and Zn into the residue fraction after pyrolysis is consistent with previous findings (although with different heating temperatures or durations) (Chen et al., 2015; Liu et al., 2016). These changes do not seem to proportionally correlate with the changes in speciation: 1) although being reduced, sulfides still account for a significant portion of total Cu, but little Cu partitioned in the oxidizable fraction, 2) sequential fractionation showed an enhancement of the Zn oxidizable fraction, while XAS fitting showed a reduction in Zn sulfides and an increase in Zn-doped ferrihydrite following pyrolysis of activated sludge. Again, these were likely caused by the intrinsic limitations of XAS LCF and sequential extraction methods as previously discussed in Section 3.2. Despite these discrepancies, the sequential extraction results demonstrated the overall stabilization of heavy metals (especially Cu) by pyrolysis.

3.4. Effects of HTC on Cu and Zn speciation

XANES and EXFAS spectra for the hydrochars and their LCA results are presented in Fig. 2 and Table 2. Despite the difference in initial composition and complex reactions under hydrothermal conditions, Cu XAS spectra of hydrochars from different feedstocks and treatment temperatures are very similar and significantly different from those of pyrochars (Fig. 2A and B). The features that distinguish the raw sludges and the hydrochars occur at ~8979 and ~8986 eV, with spectra of all hydrochars showing increasing intensity at these two positions. These two features are characteristic of the presence of Cu-Fe-sulfide minerals (Fig. S1). LCA results showed the dominance of cubanite and chalcopyrite in the hydrochars, with a combined abundance of more than 80%, compared to less than 35% in the raw sludges. Both cubanite and chalcopyrite are important Cu minerals that typically form under hydrothermal conditions and intergrowth of these two minerals is commonly found (Pruseth et al., 1999; Schwartz, 1927). Considering the presence of abundant Fe and S in the samples and the nature of hydrothermal conditions, the formation of these minerals during HTC treatment is reasonable. The results suggest that Cu-Fe-sulfide minerals, instead of pure Cu sulfides, are stable Cu phases under the tested hydrothermal conditions.

Regarding the effects of HTC on Zn, the changes following HTC are less significant than those for Cu (Fig. 2C). The most significant changes are observed for HTC of anaerobic sludge at 225 °C, with the abundance of Zn sulfides (wurtzite) increasing from 79% in the raw sludge to 94% in the char. Zn-doped ferrihydrite and hopeite may be stable under the hydrothermal conditions, and little Zn was dissolved and transformed into sulfides. Spectromicroscopy results

of the hydrochars from 225 °C showed no substantial changes in the morphology and distribution of Zn and Cu particulates (Fig. 3 Panels C1-C3 for SHTC225, Fig. S4 Panels C1-C3 for AHTC225). LCA of the μ-XANES data showed that the trends of Cu and Zn speciation evolution weresimilar to bulk XAS analysis on the samples following HTC treatment (more metal sulfides formed after HTC) (Tables S3 and S4).

Although total S content also decreased during HTC (similar to the effects of pyrolysis) (Fig. 1), the predominance of Cu and Zn sulfide species after HTC treatment suggests that these inorganic sulfides are relatively stable under hydrothermal conditions. Under hydrothermal condition, sulfide species can be released from organic structures and precipitate with chalcophile elements such as Cu and Zn (Schulte, 2010). Formation of metal sulfides under hydrothermal conditions is common in geological settings, where metal sulfide ores form (Hemley et al., 1992). Results from this study suggest that S controls the speciation of chalcophile metals during hydrothermal treatments of sewage sludge.

In terms of metal mobility as assessed by sequential extraction, following HTC treatments, the soluble/exchangeable and reducible Cu fractions became negligible (<3 and 6%, respectively) and the residual fraction significantly increased, similar to the effect of pyrolysis (Fig. 4). Although the absolute metal content in the oxidizable fraction remained mostly unchanged, the relative abundance actually decreased following HTC (from 54% in the feedstocks to 29–42% in hydrochars) (Fig. 4A). The effect was similar for both activated and anaerobic sludges. XAS fitting showed that Cu exits predominantly as Cu-Fe-sulfide species, which can partition into both the oxidizable and residual fractions. The transformation of pure Cu-sulfides to Cu-Fe-sulfides is possibly responsible for such stabilization during extraction (since Cu-sulfides in the raw sludges may contain a portion of less stable organic Cu-sulfides). Regarding Zn, the soluble/exchangeable and reducible fractions decreased and the oxidizable fraction increased after HTC treatment (Fig. 4B). The residual fraction also increased, and was more significant for hydrochars of activated sludge than those of anaerobic sludge. Considering the limited speciation transformation revealed by Zn XAS, physical changes of the matrix might play a more important role.

In summary, HTC also stabilized heavy metals in the treatment products, although not as effective as pyrolysis under the selected conditions.

4. Conclusions

This study comparatively characterized the speciation and mobility of Cu and Zn in chars from pyrolysis and HTC treatments of both activated sludge and anaerobically digested sludge, using sequential extraction, bulk XAS, and coupled μ-XRF imaging and μ-XAS. This approach helped gain a systematic and in-depth understanding of heavy metal transformation during pyrolysis and HTC treatments of sewage sludges, which can not be achieved by sequential extraction alone. Based on the results, the following conclusions can be drawn:

(1) Combined chemical, spectroscopic, and microscopic analysis provided detailed speciation information in complex samples and enabled cross validation;
(2) Cu exists predominantly as sulfides and Zn as sulfide, phosphate, and ferrihydrite-associated species in activated sludge. Both Cu and Zn became more sulfidized after anaerobic digestion;
(3) Both Cu and Zn were desulfidized after pyrolysis treatment at 250 and 450 °C. Zn became more associated with Fe minerals, while Cu became more associated with organic matters (though uncertainty existed due to relatively poor data fitting);
(4) Despite S volatilization after HTC (similar to the effect of pyrolysis), Cu remained extensively sulfidized after HTC at 175 and 225 °C, but as existed as Cu-Fe-sulfides (chalcophile and cubanite) instead of pure Cu-sulfides, and Zn was less altered (with similar portions remained as hopeite and Fe mineral associated species);
(5) Micro-XAS analysis showed that individual particles of Cu and Zn experienced similar transformation as revealed by bulk XAS analysis;
(6) Mobility of the metals was reduced after both pyrolysis and HTC treatments, which can be attributed to the changes in metal speciation and matrix property.

Associated content

Supporting Information: XANES and EXAFS spectra of Cu and Zn reference compounds, of Fe in two raw sludges, and of Cr reference compounds and Cr-added sludge and treated products; μ-XRF images of Zn, Cu, and Fe distribution and their μ-XANES spectra at individual hot spots of anaerobic sludge and its hydrochar; Results of LCF of bulk XAS; Sequential extraction (BCR protocol) results for Cu and Zn. This material is available free of charge via the Internet at www.sciencedirect.com.

Acknowledgments

This work is supported by National Science Foundation grants #1559087, 1605692, and 1739884. We thank Brandon Brown (F. Wayne Hill Water Resources Center) for help with sewage sludge collection and Dr. Hailong Chen (Georgia Tech) for help with the thermal treatment setups. We also appreciate the support from beamline scientists Benjamin Reinhart and Sungsik Lee at APS Beamline 12BM, Courtney Roach at SSRL Beamline 2–3, and Ryan Davis at SSRL Beamline 4-1. Portions of this research were conducted at the Advanced Photon Source (APS) and Stanford Synchrotron Radiation Lightsource (SSRL). APS is a U.S. Department of Energy (DOE) Office of Science User Facility operated for the DOE Office of Science by Argonne National Laboratory under Contract No. DE-AC02-06CH11357. Use of SSRL, SLAC National Accelerator Laboratory, is supported by DOE Office of Science, Office of Basic Energy Sciences under Contract No. DE-AC02-76SF00515.

Appendix A. Supplementary data

Supplementary data related to this article can be found at https://doi.org/10.1016/j.watres.2018.01.009.

References

Atkinson, C., Fitzgerald, J., Hipps, N., 2010. Potential mechanisms for achieving agricultural benefits from biochar application to temperate soils: a review. Plant Soil 337 (1–2), 1–18.
Barber, W.P.F., 2016. Thermal hydrolysis for sewage treatment: a critical review. Water Res. 104, 53–71.
Bridle, T., Pritchard, D., 2004. Energy and nutrient recovery from sewage sludge via pyrolysis. Water Sci. Technol. 50 (9), 169–175.
Brown, M.J., Lester, J.N., 1982. Role of bacterial extracellular polymers in metal uptake in pure bacterial culture and activated sludge—I. Effects of metal concentration. Water Res. 16 (11), 1539–1548.
Chen, F., Hu, Y., Dou, X., Chen, D., Dai, X., 2015. Chemical forms of heavy metals in pyrolytic char of heavy metal-implanted sewage sludge and their impacts on leaching behaviors. J. Anal. Appl. Pyrol. 116, 152–160.
Chipasa, K.B., 2003. Accumulation and fate of selected heavy metals in a biological wastewater treatment system. Waste Manag. 23 (2), 135–143.
Christodoulou, A., Stamatelatou, K., 2016. Overview of legislation on sewage sludge management in developed countries worldwide. Water Sci. Technol. 73 (3),

453–462.
Donner, E., Brunetti, G., Zarcinas, B., Harris, P., Tavakkoli, E., Naidu, R., Lombi, E., 2013. Effects of chemical amendments on the lability and speciation of metals in anaerobically digested biosolids. Environ. Sci. Technol. 47 (19), 11157–11165.
Donner, E., Howard, D.L., Jonge, M.D.D., Paterson, D., Cheah, M.H., Naidu, R., Lombi, E., 2011. X-ray absorption and micro x-ray fluorescence spectroscopy investigation of copper and zinc speciation in biosolids. Environ. Sci. Technol. 45 (17), 7249–7257.
Donner, E., Ryan, C.G., Howard, D.L., Zarcinas, B., Scheckel, K.G., McGrath, S.P., de Jonge, M.D., Paterson, D., Naidu, R., Lombi, E., 2012. A multi-technique investigation of copper and zinc distribution, speciation and potential bioavailability in biosolids. Environ. Pollut. 166 (0), 57–64.
Dunnette, D.A., Chynoweth, D.P., Mancy, K.H., 1985. The source of hydrogen sulfide in anoxic sediment. Water Res. 19 (7), 875–884.
Escala, M., Zumbühl, T., Koller, C., Junge, R., Krebs, R., 2013. Hydrothermal carbonization as an energy-efficient alternative to established drying technologies for sewage sludge: a feasibility study on a laboratory scale. Energy Fuel. 27 (1), 454–460.
Escala, M., Zumbühl, T., Koller, C., Junge, R., Krebs, R., 2012. Hydrothermal carbonization as an energy-efficient alternative to established drying technologies for sewage sludge: a feasibility study on a laboratory scale. Energy Fuel. 27 (1), 454–460.
García-Delgado, M., Rodríguez-Cruz, M.S., Lorenzo, L.F., Arienzo, M., Sánchez-Martín, M.J., 2007. Seasonal and time variability of heavy metal content and of its chemical forms in sewage sludges from different wastewater treatment plants. Sci. Total Environ. 382 (1), 82–92.
Goldschmidt, V.M., 1937. The principles of distribution of chemical elements in minerals and rocks. The seventh Hugo Muller Lecture, delivered before the Chemical Society on March 17th, 1937. J. Chem. Soc. 0, 655–673.
Hemley, J.J., Cygan, G.L., Fein, J.B., Robinson, G.R., d'Angelo, W.M., 1992. Hydrothermal ore-forming processes in the light of studies in rock-buffered systems; I, Iron-copper-zinc-lead sulfide solubility relations. Econ. Geol. 87 (1), 1–22.
Hossain, M.K., Strezov, V., Yin Chan, K., Nelson, P.F., 2010. Agronomic properties of wastewater sludge biochar and bioavailability of metals in production of cherry tomato (Lycopersicon esculentum). Chemosphere 78 (9), 1167–1171.
Huang, H.-j., Yuan, X.-z., 2016. The migration and transformation behaviors of heavy metals during the hydrothermal treatment of sewage sludge. Bioresour. Technol. 200, 991–998.
Huang, R., Tang, Y., 2016. Evolution of phosphorus complexation and mineralogy during (hydro)thermal treatments of activated and anaerobically digested sludge: insights from sequential extraction and P K-edge XANES. Water Res. 100, 439–447.
Huang, R., Tang, Y., 2015. Speciation dynamics of phosphorus during (Hydro)Thermal treatments of sewage sludge. Environ. Sci. Technol. 49 (24), 14466–14474.
Isa, Z., Grusenmeyer, S., Verstraete, W., 1986. Sulfate reduction relative to methane production in high-rate anaerobic digestion: microbiological aspects. Appl. Environ. Microbiol. 51 (3), 580–587.
Jin, J., Li, Y., Zhang, J., Wu, S., Cao, Y., Liang, P., Zhang, J., Wong, M.H., Wang, M., Shan, S., Christie, P., 2016. Influence of pyrolysis temperature on properties and environmental safety of heavy metals in biochars derived from municipal sewage sludge. J. Hazard Mater. 320, 417–426.
Kim, B., Levard, C., Murayama, M., Brown, G.E., Hochella, M.F., 2014a. Integrated approaches of X-ray absorption spectroscopic and electron microscopic techniques on zinc speciation and characterization in a final sewage sludge product. J. Environ. Qual. 43 (3), 908–916.
Kim, B., Miller, J.H., Monsegue, N., Levard, C., Hong, Y., Hull, M.S., Murayama, M., Brown, G.E., Vikesland, P.J., Knocke, W.R., Pruden, A., Hochella, M.F., 2015. Silver sulfidation in thermophilic anaerobic digesters and effects on antibiotic resistance genes. Environ. Eng. Sci. 33 (1), 1–10.
Kim, D., Lee, K., Park, K.Y., 2014b. Hydrothermal carbonization of anaerobically digested sludge for solid fuel production and energy recovery. Fuel 130 (0), 120–125.
Koppelaar, R.H.E.M., Weikard, H.P., 2013. Assessing phosphate rock depletion and phosphorus recycling options. Global Environ. Change 23 (6), 1454–1466.
Lake, D.L., Kirk, P.W.W., Lester, J.N., 1984. Fractionation, characterization, and speciation of heavy metals in sewage sludge and sludge-amended soils: a Review1. J. Environ. Qual. 13, 175–183.
Lawrence, A.W., McCarty, P.L., 1965. The role of sulfide in preventing heavy metal toxicity in anaerobic treatment. J. (Water Pollut. Control Fed.) 392–406.
Legros, S., Levard, C., Marcato-Romain, C.E., Guiresse, M., Doelsch, E., 2017. Anaerobic digestion alters copper and zinc speciation. Environ. Sci. Technol. 51 (18), 10326–10334. https://doi.org/10.1021/acs.est.7b01662.
Leng, L., Yuan, X., Huang, H., Jiang, H., Chen, X., Zeng, G., 2014. The migration and transformation behavior of heavy metals during the liquefaction process of sewage sludge. Bioresour. Technol. 167, 144–150.
Li, L., Xu, Z.R., Zhang, C.L., Bao, J.P., Dai, X.X., 2012. Quantitative evaluation of heavy metals in solid residues from sub- and super-critical water gasification of sewage sludge. Bioresour. Technol. 121, 169–175.
Liu, X., Wang, Y., Gui, C., Li, P., Zhang, J., Zhong, H., Wei, Y., 2016. Chemical forms and risk assessment of heavy metals in sludge-biochar produced by microwave-induced low temperature pyrolysis. RSC Advances 6 (104), 101960–101967.
Lombi, E., Donner, E., Taheri, S., Tavakkoli, E., Jämting, Å.K., McClure, S., Naidu, R., Miller, B.W., Scheckel, K.G., Vasilev, K., 2013. Transformation of four silver/silver chloride nanoparticles during anaerobic treatment of wastewater and post-processing of sewage sludge. Environ. Pollut. 176, 193–197.
Lombi, E., Donner, E., Tavakkoli, E., Turney, T.W., Naidu, R., Miller, B.W., Scheckel, K.G., 2012. Fate of zinc oxide nanoparticles during anaerobic digestion of wastewater and post-treatment processing of sewage sludge. Environ. Sci. Technol. 46 (16), 9089–9096.
Ma, R., Levard, C., Judy, J.D., Unrine, J.M., Durenkamp, M., Martin, B., Jefferson, B., Lowry, G.V., 2014a. Fate of zinc oxide and silver nanoparticles in a pilot wastewater treatment plant and in processed biosolids. Environ. Sci. Technol. 48 (1), 104–112.
Ma, R., Stegemeier, J., Levard, C., Dale, J.G., Noack, C.W., Yang, T., Brown, G.E., Lowry, G.V., 2014b. Sulfidation of copper oxide nanoparticles and properties of resulting copper sulfide. Environmental Science: Nano 1 (4), 347–357.
Malghani, S., Gleixner, G., Trumbore, S.E., 2013. Chars produced by slow pyrolysis and hydrothermal carbonization vary in carbon sequestration potential and greenhouse gases emissions. Soil Biol. Biochem. 62, 137–146.
Manara, P., Zabaniotou, A., 2012. Towards sewage sludge based biofuels via thermochemical conversion - a review. Renew. Sustain. Energy Rev. 16 (5), 2566–2582.
Mitrano, D.M., Rimmele, E., Wichser, A., Erni, R., Height, M., Nowack, B., 2014. Presence of nanoparticles in wash water from conventional silver and nano-silver textiles. ACS Nano 8 (7), 7208–7219.
Mossop, K.F., Davidson, C.M., 2003. Comparison of original and modified BCR sequential extraction procedures for the fractionation of copper, iron, lead, manganese and zinc in soils and sediments. Anal. Chim. Acta 478 (1), 111–118.
Parkhurst, D.L., Appelo, C., 1999. User's Guide to PHREEQC (Version 2): a Computer Program for Speciation, Batch-reaction, One-dimensional Transport, and Inverse Geochemical Calculations. USGS Report.
Pruseth, K.L., Mishra, B., Bernhardt, H.J., 1999. An-experimental study on cubanite irreversibility: implications for natural chalcopyrite-cubanite intergrowths. Eur. J. Mineral 11 (3), 471–476.
Rathnayake, S., Unrine, J.M., Judy, J., Miller, A.-F., Rao, W., Bertsch, P.M., 2014. Multitechnique investigation of the pH dependence of phosphate induced transformations of ZnO nanoparticles. Environ. Sci. Technol. 48 (9), 4757–4764.
Ravel, á., Newville, M., 2005. ATHENA, ARTEMIS, HEPHAESTUS: data analysis for X-ray absorption spectroscopy using IFEFFIT. J. Synchrotron Radiat. 12 (4), 537–541.
Reeder, R.J., Schoonen, M.A.A., Lanzirotti, A., 2006. Metal speciation and its role in bioaccessibility and bioavailability. Rev. Mineral. Geochem. 64 (1), 59–113.
Rogers, H.R., 1996. Sources, behaviour and fate of organic contaminants during sewage treatment and in sewage sludges. Sci. Total Environ. 185 (1–3), 3–26.
Schulte, M., 2010. Organic sulfides in hydrothermal solution: standard partial molal properties and role in organic geochemistry of hydrothermal environments. Aquat. Geochem. 16 (4), 621–637.
Schwartz, G.M., 1927. Intergrowths of chalcopyrite and cubanite; experimental proof of the origin of intergrowths and their bearing on the geologic thermometer. Econ. Geol. 22 (1), 44–61.
Shao, J., Yuan, X., Leng, L., Huang, H., Jiang, L., Wang, H., Chen, X., Zeng, G., 2015. The comparison of the migration and transformation behavior of heavy metals during pyrolysis and liquefaction of municipal sewage sludge, paper mill sludge, and slaughterhouse sludge. Bioresour. Technol. 198, 16–22.
Shi, W., Liu, C., Ding, D., Lei, Z., Yang, Y., Feng, C., Zhang, Z., 2013. Immobilization of heavy metals in sewage sludge by using subcritical water technology. Bioresour. Technol. 137, 18–24.
Spinosa, L., 2004. From sludge to resources through biosolids. Water Sci. Technol. 50 (9), 1–9.
Stasinakis, A.S., Thomaidis, N.S., Mamais, D., Karivali, M., Lekkas, T.D., 2003. Chromium species behaviour in the activated sludge process. Chemosphere 52 (6), 1059–1067.
Stephenson, T., Lester, J.N., 1987. Heavy metal behaviour during the activated sludge process I. Extent of soluble and insoluble metal removal. Sci. Total Environ. 63, 199–214.
Sterritt, R., Lester, J., 1984. Significance and behaviour of heavy metals in waste water treatment processes III. Speciation in waste waters and related complex matrices. Sci. Total Environ. 34 (1–2), 117–141.
vom Eyser, C., Palmu, K., Otterpohl, R., Schmidt, T.C., Tuerk, J., 2015a. Determination of pharmaceuticals in sewage sludge and biochar from hydrothermal carbonization using different quantification approaches and matrix effect studies. Anal. Bioanal. Chem. 407 (3), 821–830.
vom Eyser, C., Palmu, K., Schmidt, T.C., Tuerk, J., 2015b. Pharmaceutical load in sewage sludge and biochar produced by hydrothermal carbonization. Sci. Total Environ. 537, 180–186.
Wang, L., Li, A., 2015. Hydrothermal treatment coupled with mechanical expression at increased temperature for excess sludge dewatering: the dewatering performance and the characteristics of products. Water Res. 68, 291–303.
Wang, L.P., Zhang, L., Li, A.M., 2014. Hydrothermal treatment coupled with mechanical expression at increased temperature for excess sludge dewatering: influence of operating conditions and the process energetics. Water Res. 65, 85–97.
Wang, X., McCarty, P.L., Liu, J., Ren, N.-Q., Lee, D.-J., Yu, H.-Q., Qian, Y., Qu, J., 2015. Probabilistic evaluation of integrating resource recovery into wastewater treatment to improve environmental sustainability. Proc. Natl. Acad. Sci. Unit. States Am. 112 (5), 1630–1635.
Webb, S., 2005. SIXpack: a graphical user interface for XAS analysis using IFEFFIT. Phys. Scripta T115, 1011–1014.
Westerhoff, P., Lee, S., Yang, Y., Gordon, G.W., Hristovski, K., Halden, R.U., Herckes, P., 2015. Characterization, recovery opportunities, and valuation of metals in

municipal sludges from U.S. Wastewater treatment plants nationwide. Environ. Sci. Technol. 49 (16), 9479–9488.
Withers, P.J.A., Elser, J.J., Hilton, J., Ohtake, H., Schipper, W.J., van Dijkf, K.C., 2015. Greening the global phosphorus cycle: how green chemistry can help achieve planetary P sustainability. Green Chem. 17 (4), 2087–2099.
Wu, H., Li, M., Zhang, L., Sheng, C., 2016. Research on the stability of heavy metals (Cu, Zn) in excess sludge with the pretreatment of thermal hydrolysis. Water Sci. Technol. 73 (4), 890–898.
Yuan, X.Z., Huang, H.J., Zeng, G.M., Li, H., Wang, J.Y., Zhou, C.F., Zhu, H.N., Pei, X.K., Liu, Z.F., Liu, Z.T., 2011. Total concentrations and chemical speciation of heavy metals in liquefaction residues of sewage sludge. Bioresour. Technol. 102 (5), 4104–4110.
Yuan, X.Z., Leng, L.J., Huang, H.J., Chen, X.H., Wang, H., Xiao, Z.H., Zhai, Y.B., Chen, H.M., Zeng, G.M., 2015. Speciation and environmental risk assessment of heavy metal in bio-oil from liquefaction/pyrolysis of sewage sludge. Chemosphere 120, 645–652.
Zhang, J., Zuo, W., Tian, Y., Chen, L., Yin, L., Zhang, J., 2017. Sulfur transformation during microwave and conventional pyrolysis of sewage sludge. Environ. Sci. Technol. 51 (1), 709–717.
Zhang, Q., Zhang, L., Sang, W., Li, M., Cheng, W., 2016. Chemical speciation of heavy metals in excess sludge treatment by thermal hydrolysis and anaerobic digestion process. Desalination WaterTreat. 57 (27), 12770–12776.
Zhao, P.T., Shen, Y.F., Ge, S.F., Yoshikawa, K., 2014. Energy recycling from sewage sludge by producing solid biofuel with hydrothermal carbonization. Energy Convers. Manag. 78, 815–821.